IEEE Access
Multidisciplinary | Rapid Review | Open Access Journal

Received 6 December 2022, accepted 19 December 2022, date of publication 12 January 2023, date of current version 19 January 2023.

Digital Object Identifier 10.1109/ACCESS.2023.3236606

RESEARCH ARTICLE

New Class of Cosine-Sum Windows

TOMOYA YAMAOKA[1] AND SATOSHI KAGEME[2]
[1]Information Technology Research and Development Center, Mitsubishi Electric Corporation, Kamakura 247-8501, Japan
[2]Kamakura Works, Mitsubishi Electric Corporation, Kamakura 247-8520, Japan

Corresponding author: Tomoya Yamaoka (yamaoka.tomoya@ab.mitsubishielectric.co.jp)

ABSTRACT Window functions are required to achieve excellent frequency resolution, peak sidelobe ratio, and sidelobe decay. The cosine-sum window function satisfies these requirements. However, conventional cosine-sum windows limit the number of terms and coefficient values. Therefore, this study proposes a new class of cosine-sum windows that has more terms than those in the conventional cosine-sum window and considers positive and negative coefficients. For such windows, we present three design examples. The first is a window function with low sidelobe decay, which reduce the sidelobes by adding correction terms to the conventional windows without damaging the sidelobe decay. The second is a window function that improves the frequency resolution by emphasizing the discontinuities of the extracted signal. The third is a window function that reduces sidelobes further without deteriorating the frequency resolution by adding correction terms to the window functions, which are designed in advance. We confirmed the effectiveness of these examples of the proposed window function.

INDEX TERMS Window function, cosine-sum windows, raised-cosine windows, Hann window, Blackman window.

I. INTRODUCTION

In signal processing, a window function is used to reduce the sidelobes generated by the Gibbs phenomenon in accordance with the frequency transform [1]. For applications using the window function, we raise the suppression of co-channel interference [2], harmonic analysis in real-time systems [3], satellite altimeter waveforms [4], radar systems [5], [6], [7], sensor arrays [8], and audio systems [9], [10]. The window function has been studied in various ways [11], [12], [13], [14], [15], [16], [17], [18], [19], [20], [21], [22].

When evaluating window function, the following three perspectives are important.

1) Frequency resolution is good.
2) Peak sidelobe ratio (PSLR) is low.
3) Sidelobe decay is excellent.

The window function was designed according to these evaluation parameters. Typical window functions are the Hamming, Hann, Kaiser, Gaussian, and Chebyshev windows. The Hamming and Hann windows are composed of a constant term and cosine function. In the frequency region, the sidelobes of the constant term and cosine function cancel each other and reduce. In particular, the PSLR of the Hamming window and the sidelobe decay of the Hann window are good. The Kaiser, Gaussian, and Chebyshev windows can be designed using a parameter with a trade-off between the frequency resolution and sidelobe characteristics. On the other hand, cosine-sum windows were proposed by incorporating the properties of the Hamming window and Hann window to design a trade-off between the frequency resolution and sidelobe characteristics [1]. The cosine-sum window functions are expressed as follows:

$$w_{\mathrm{conv}}(x) = \Sigma_{k=0}^{K} a_k \cos(2\pi kx) - 0.5 \leq x \leq 0.5, \qquad (1)$$

where k and K are the natural numbers and $a_k \geq 0$. We can design a window function flexibly using a_k.

Here, we discuss studies of window functions that focus on sidelobe decay. Reference [23], [24], and [25] indicate window functions, which are based on the polynomial, Gamma function, and cosine-sum windows (sine-sum windows), respectively, and are excellent in sidelobe decay, although they exhibit high PSLR. Reference [26] shows window functions with multiple values of -12 dB/oct. This indicates that the window function can be designed flexibly to achieve the

The associate editor coordinating the review of this manuscript and approving it for publication was Fabrizio Santi.

desired frequency resolution and PSLR without impairing the sidelobe decay. With this in mind, we designed functions to achieve excellent frequency resolution and PSLR in each sidelobe decay. Specifically, we present design examples at −6, −12, −18, −24, −30 and −36 dB/oct. Recently, several window functions that achieve good performance have been proposed [27], [28], [29]. In contrast, our proposed windows can design sidelobe decay or improve frequency resolution with low peak sidelobes.

In this study, we expanded the cosine-sum windows to design the window function above. Specifically, it is expressed as follows.

$$w_{\mathrm{pro}}(x) = \Sigma_{l=0}^{L} b_l \cos(\pi l x) \tag{2}$$

l and L are natural numbers and b_l is a real number. To simplify the window function analysis, the length of the window is assumed to be 1. However, it can be scaled to any desired signal length using mathematical treatment of the variables. The proposed window has a large number of cosine functions, and coefficient b_l has a positive or negative value. For such windows, we present three design examples. The first is a window function that reduces sidelobes with low sidelobe decay. We demonstrate the window functions to reduce the sidelobes by adding correction terms to the conventional windows without damaging the sidelobe decay. Furthermore, we show design examples that can reduce peak sidelobes with a slight deterioration of the frequency resolution, while the sidelobe decay was the same. The second is a window function that improves the frequency resolution. We propose window functions to improve the frequency resolution by emphasizing the discontinuities of the extracted signal. In addition, we present design examples that reduced the PSLR. The third is a window function designed in advance to further reduce sidelobes. We added correction terms to the window functions at −6 and −12 dB/oct, which were designed in advance to further reduce the sidelobes without deteriorating frequency resolution. The first, second, and third window functions are presented in Sections II, III, and IV, respectively. Each section shows the design guidelines, proposed windows, and their evaluation results.

II. WINDOW FUNCTIONS REDUCING THE SIDELOBES WITH LOW SIDELOBE DECAY

A. DESIGN GUIDELINE

In cosine-sum windows, the Hann window and Blackman window exhibit excellent sidelobe decay. In the Hann window, the sidelobe decay is −18 dB/oct. On the other hand, the Blackman window also has a sidelobe decay of −18 dB/oct. The Blackman window achieves a low PSLR by adding terms that reduce the sidelobe to the Hann window, where the sidelobe decay is −18 dB/oct. Using this principle, we can design window functions that have both a low PSLR and excellent sidelobe decay; however, it deteriorates the frequency resolution. Better window functions can be designed, if there is a reduction method for sidelobes that solves this problem.

In this section, we propose an excellent sidelobe reduction method with a low sidelobe decay based on the window function presented in [25]. In [25], window functions of −18, −24, −30, and −36 dB/oct. are shown. First, we add correction terms that reduce sidelobes without damaging the sidelobe decay of conventional windows. However, the frequency resolution deteriorates in these window functions. Therefore, we also propose window functions that add correction terms to reduce the PSLR while reducing the deterioration of the frequency resolution. The window functions designed in these ways exhibit sidelobe decay of −18, −24, −30, and −36 dB/oct; however, the sidelobes are reduced compared to conventional windows.

B. PROPOSED WINDOWS

First, the basic functions of the window that achieve good sidelobe decay are provided as follows:

$$\begin{aligned} f_1(x,k) = {} & (\cos((-2+2k)\pi x) + 2\cos(2k\pi x) \\ & + \cos((2+2k)\pi x))/4 \end{aligned} \tag{3}$$

$$\begin{aligned} f_2(x,k) = {} & (\cos((-3+2k)\pi x) + 3\cos((-1+2k)\pi x) \\ & + 3\cos((1+2k)\pi x) + \cos((3+2k)\pi x))/8 \end{aligned} \tag{4}$$

$$\begin{aligned} f_3(x,k) = {} & (\cos((-4+2k)\pi x) + 4\cos((-2+2k)\pi x) \\ & + 6\cos(2k\pi x) + 4\cos((2+2k)\pi x) \\ & + \cos((4+2k)\pi x))/16 \end{aligned} \tag{5}$$

$$\begin{aligned} f_4((x,k) = {} & (\cos((-5+2k)\pi x) + 5\cos((-3+2k)\pi x) \\ & + 10\cos((-1+2k)\pi x) + 10\cos((1+2k)\pi x) \\ & + 5\cos((3+2k)\pi x) + \cos((5+2k)\pi x))/32 \end{aligned} \tag{6}$$

Each $f_i(x,k)$ $(i = 1,2,3,4)$ exhibit a side-lobe decay of −18, −24, −30, and −36 dB/oct, respectively. Such low sidelobe decay can be achieved by repeatedly synthesizing the adjacent cosine component with equal gains. This process is the reverse of Pascal's triangle expansion. Therefore, the coefficients of $f_i(x,k)$ follow Pascal's triangle.

Thus, the conventional window i described in [25] can be expressed as follows:

$$w_{\mathrm{convi}}(x) = f_i(x,0) \tag{7}$$

The Hann window is a conventional window 1. The conventional windows i achieve sidelobe decay of −18, −24, −30, and −36 dB/oct, respectively, but with a higher PSLR. For conventional window i, we add $f_i(x,1)$ with the same sidelobe decay to reduce the sidelobes. Specifically, the proposed window i, a is expressed as follows:

$$w_{\mathrm{pro}i,a}(x) = (1-\alpha) w_{\mathrm{conv}i}(x) + \alpha f_i(x,1) \tag{8}$$

where α is real number. Although $f_i(x,1)$ exhibits the same sidelobe decay as $w_{\mathrm{conv}i}(x)$ and reduces the sidelobes, it degrades the frequency resolution. Therefore, in the proposed window i,a, the frequency resolution deteriorates;

TABLE 1. Evaluation results of proposed windows 1, 2, 3, and 4.

window	α/β	γ	3dB width	Main-lobe width	PSLR [dB]	ISLR [dB]
Rectangular	-	-	0.888	2	-13.26	-9.68
Hann	-	-	1.438	4	-31.47	-32.88
Proposed1,b	0.031	-	1.451	4.24	-38.05	-36.94
Proposed 1,c	0.06	0.02	1.465	4.44	-42.7	-40
Blackman	-	-	1.641	6	-58.11	-57.16
Conventional 2	-	-	1.656	5	-39.3	-41.65
Proposed 2,b	0.02	-	1.668	5.319	-47.5	-47.44
Proposed 2,c	0.039	0.009	1.979	5.532	-52.2	-51.35
Proposed 2,a	0.323	-	1.853	7	-73.57	-72.89
Conventional 3	-	-	1.85	6	-46.74	-49.78
Proposed 3,b	0.014	-	1.86	6.382	-56.25	-57.01
Proposed 3,c	0.03	0.006	1.87	6.619	-62.61	-62.08
Proposed 3,a	0.288	-	2.012	8	-82.56	-82.43
Conventional 4	-	-	2.026	7	-53.93	-57.52
Proposed 4,b	0.01	-	2.034	7.41	-64.68	-65.85
Proposed 4,c	0.024	0.004	2.044	7.731	-72.27	-72.15
Proposed 4,a	0.259	-	2.163	9	-91.28	-91.38

however, the sidelobes are reduced as compared to the conventional window i. α can be set according to the desired frequency resolution. We set α to minimize the PSLR. $w_{\mathrm{pro1},a}(x)$ is the Blackman window function. Therefore, the design principle of the proposed window i, a is based on that of the Blackman window.

Furthermore, we propose the window functions, in which the frequency resolutions are less deteriorated, sidelobes are reduced, and sidelobe decays are excellent. In $w_{\mathrm{conv}i}(x)$, the frequency resolution deteriorates because of the term $f_i(x,1)$. Therefore, we propose the proposed window i, c to reduce the PSLR by including the terms $f_i(x,2)$ and $-f_i(x,3)$ without $f_i(x,1)$. They are given as follows:

$$w_{\mathrm{proi},c}(x) = (1-\beta+\gamma)w_{\mathrm{conv}i}(x) + \beta f_i(x,2) - \gamma f_i(x,3), \tag{9}$$

where β and γ are real numbers. Because β and γ are small and the main lobes of $f_i(x,2)$ and $-f_i(x,3)$ are separated from that of $w_{\mathrm{conv}i}(x)$, the deterioration in the frequency resolution is small. $f_i(x,2)$ primarily reduces the first sidelobe of $w_{\mathrm{conv}i}(x)$. -$f_i(x,3)$ mainly increases the first side lobes but decreases the second side lobe. Therefore, as a result, the first and second sidelobes are reduced in the proposed window i, c. In this study, β and γ are set such that the first, second, and third sidelobes are at the same level. At this time, a feature of the proposed windows is that the coefficients include negative values. Furthermore, the case in which $\gamma = 0$, is defined as the proposed window i, b. The proposed window i, b is a window function with the reduced first sidelobe. We set β such that the first and second sidelobes are at the same level. In the next subsection, we describe the design and evaluation of the proposed windows.

C. EVALUATION RESULTS

In this subsection, the evaluation results for the proposed windows are presented. Table 1 lists the design and evaluation results of the proposed windows. Note that the design results are based on a trial-and-error approach. To understand the performance of the proposed windows, we evaluated the 3 dB width, PSLR, and integrated side-lobe ratio (ISLR). The power profiles obtained by transforming the proposed windows to the frequency region were used for the evaluation. The evaluation results are listed in Table 1. We measured the 3 dB width and width of the main lobe. The PSLR is the maximum power of the sidelobes in the normalized power profile. The ISLR was derived by determining the total power ratio of the sidelobes to the main lobe.

Table 1 lists the design and evaluation results of the proposed windows. Although the proposed window i, a improves the PSLR and ISLR of conventional windows, the frequency resolution deteriorates. On the other hand, in the proposed windows i, b and i, c, the deterioration of the frequency resolution is small; however, the PSLR and ISLR are reduced.

In addition, normalized power profiles were obtained to confirm the aspects of the sidelobes. The horizontal and vertical axes represent the frequency-normalized by time, and the normalized power, respectively. To confirm the sidelobe decay by comparison, Fig.1 shows the profiles of the conventional window i and the sinc function. The profiles of the conventional window i and sinc function are represented by red, blue, green, yellow, and gray lines. Next, to compare the conventional and proposed windows, the profiles of -18 dB/oct., -24 dB/oct., -30 dB/oct., -36 dB/oct. are shown in Figs. 2, 3, 4 and 5, respectively. The line colors of the conventional window i are the same as those in Fig.1. The profiles of the proposed windows i, a, i, b, and i, c are shown in black, gray, and light-gray, respectively. Each proposed window achieves the same sidelobe decay as the conventional windows. In the proposed window i, b, the first and second side sidelobes were at the same level. In the proposed window i, c, the first, second, and third sidelobes were at the same level. Shaping reduces the PSLR. In particular, the proposed

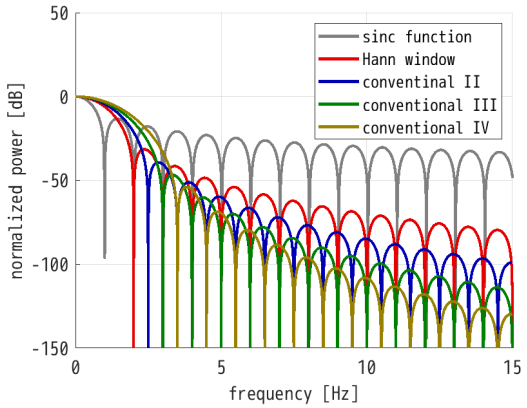

FIGURE 1. Power profile of the conventional windows.

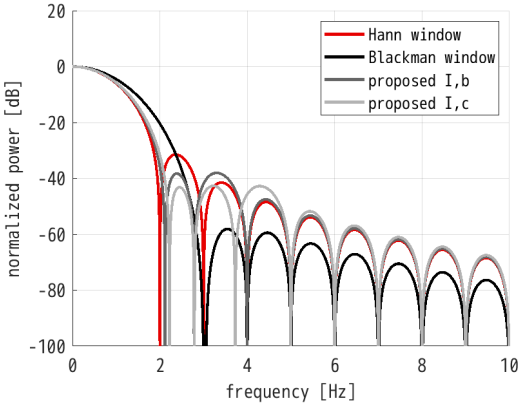

FIGURE 2. Power profile of −18dB/oct.

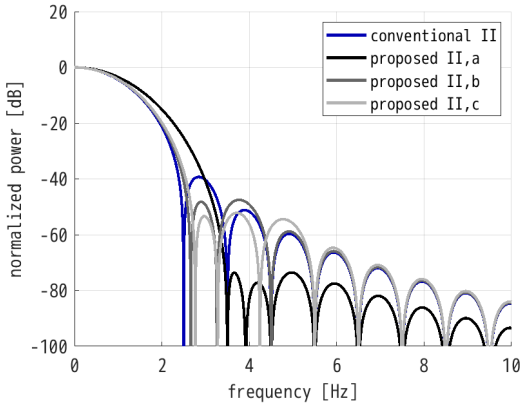

FIGURE 3. Power profile of −24dB/oct.

window i, c has lower peak sidelobes than the second sidelobes in conventional window i. The proposed window i, a, reduces the sidelobe level; however, the frequency resolution deteriorates.

III. WINDOW FUNCTIONS IMPROVING THE FREQUENCY RESOLUTION

A. DESIGN GUIDELINE

The window function reduces sidelobes at the cost of degrading the frequency resolution by ensuring signal continuity.

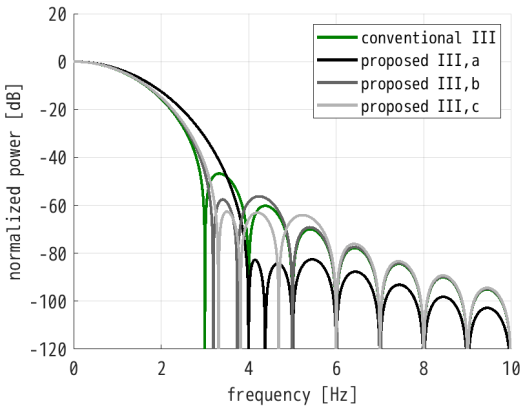

FIGURE 4. Power profile of −30dB/oct.

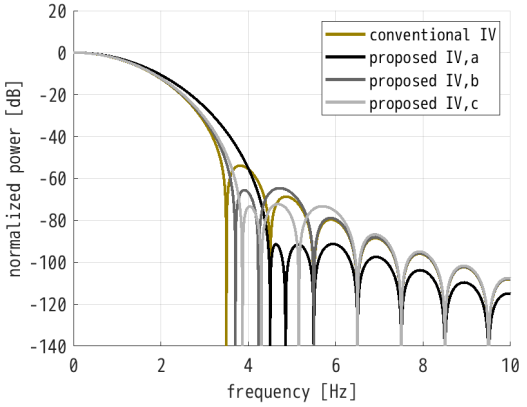

FIGURE 5. Power profile of −36dB/oct.

In this section, we discuss the design of a window function to improve the frequency resolution by emphasizing the signal discontinuity. To emphasize the discontinuity, the proposed windows were relatively high at both ends. Such a discontinuity causes an increase in the sidelobes of the frequency region. However, in contrast to the normal window function, an improvement in the frequency resolution can be expected. Furthermore, for such a window function, the result of the modification to reduce the PSLR is also shown. From the evaluation results, we show that such a window function can simultaneously improve the frequency resolution and PSLR. Notably that we assume the use of digital signal processing. We consider that performance was mostly degraded because of the Gibbs phenomenon.

B. PROPOSED WINDOWS

In this section, we propose window functions to improve frequency resolution. The usual window function reduces the sidelobes in the frequency region by ensuring continuity at both ends of the waveform; however, the frequency resolution deteriorates. In other words, to improve the frequency resolution, the discontinuity at both ends of the waveform must be emphasized. If we design a window function that emphasizes discontinuity at both ends of the waveform, we add a

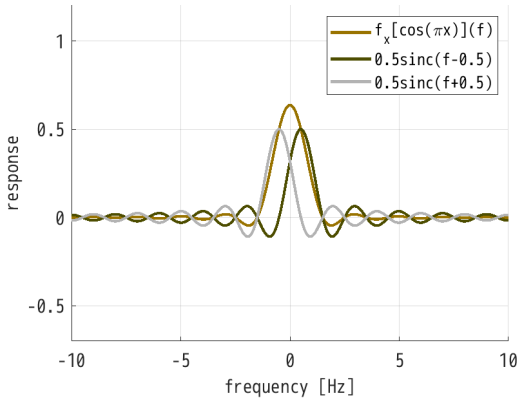

FIGURE 6. Frequency response of $\cos(\pi x)$.

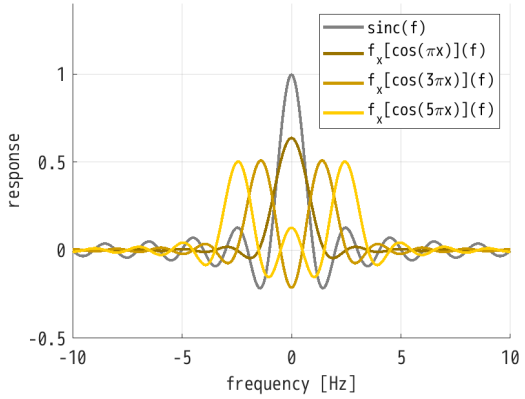

FIGURE 7. Frequency response of $\cos(\pi x)$.

function that reduces the center of the window. However, it is necessary to consider that the sidelobes increase owing to the addition of such a function. Therefore, the function to be added must have low sidelobes in the frequency region. In this study, $\cos(\pi x)$ $(-0.5 \leq x \leq 0.5)$ is used for this purpose. As $\cos(\pi x) = (e^{j\pi x} + e^{-j\pi x})/2$, the frequency response of $\cos(\pi x)$ is the sum of the two sinc functions shifted by $\pm 1/2$. Fig.6 shows the frequency response of $\cos(\pi x)$. $f_x[](f)$ represents the transformation from x to the frequency f, where the vertical axis represents the response, the horizontal axis represents the frequency normalized by time, the gray line represents $\mathrm{sinc}(f \pm 1/2)$, and the yellow line represents $f_x[\cos(\pi x)](f)$. Each side lobe of the two sinc functions shifted by $\pm 1/2$ has opposite signs. The sidelobes of $f_x[\cos(\pi x)](f)$ obtained by superimposing both are reduced. The sidelobe decay of $\cos(\pi x)$ was -12 dB/oct. Considering that the sidelobe decay of the sinc function is -6 dB/oct., $\cos(\pi x)$ is suitable for designing the proposed window. However, as described below, this term reduces the size of the main lobe.

Based on the above, we designed window functions that emphasize waveform discontinuity. We can express the proposed window 5 as follows:

$$w_{\mathrm{pro5}}(x) = 1 - \alpha cos(\pi x). \tag{10}$$

α is a real number with $0 \leq \alpha < 1$.

The proposed window 5 has a problem in that the sidelobes in the frequency region are high owing to the discontinuity. Therefore, the proposed window 5 is corrected to reduce the PSLR. To reduce the peak sidelobes, we focus on $\cos((2k+1)\pi x)$. $f_x[\cos((2k+1)\pi x)](f)$ is the sum of two sinc functions shifted by $\pm(k+1/2)$, which reduces the sidelobes as well as $\cos(\pi x)$. The sidelobe decay is given by -12 dB/oct. Because $f_x[\cos((2k+1)\pi x)](f)$ is the sum of the two sinc functions shifted by $\pm(k+1/2)$, the center of the main lobes is located at $f = \pm(k+1/2)$. In contrast, the l-th sidelobe of the sinc function is located approximately $\pm(l+1/2)$. Therefore, if $k = l$, the l-th sidelobe of the sinc function is included in the main lobes of $f_x[\cos((2k+1)\pi x)](f)$. The proposed reduction in PSLR is based on this property.

Next, we explain windows 6 and 7, which reduce the PSLR of window 5. To understand the principle of the proposed reducing PSLR, Fig.7 shows the sinc functions, $f_x[\cos(\pi x)](f)$, $f_x[\cos(3\pi x)](f)$, and $f_x[\cos(5\pi x)](f)$. In Fig.7, the vertical axis represents the response, the horizontal axis represents the frequency normalized by time, the gray line represents the sinc function, and the yellow line represents $f_x[\cos((2k+1)\pi x)](f)$. The first and second side lobes are included in the mainlobes of $f_x[\cos(3\pi x)](f)$ and $f_x[\cos(5\pi x)](f)$, respectively. Because the sign of the l-th sidelobe of the sinc function is given by $(-1)^l$, the first and second sidelobes can be reduced by $\cos(3\pi x)$ and $\cos(5\pi x)$, respectively. Therefore, we design a window function that reduces the PSLR with respect to the proposed window 5 as

$$w_{\mathrm{pro7}}(x) = 1 - \alpha\cos(\pi x) + \beta\cos(3\pi x) - \gamma\cos(5\pi x) \tag{11}$$

where β and γ are real numbers with $\beta \geq 0$ and $\gamma \geq 0$. Let the proposed window 6 be at $\gamma = 0$, and window 7 be at the others. In the design of proposed window 6, β is set such that the first and second sidelobes in the frequency region are at the same level. In the design of the proposed window 7, β and γ are set such that the first, second, and third sidelobes in the frequency region are at the same level. We reduced the PSLR using this design. This correction deteriorates the frequency resolution; however, it provides window functions that exhibit both good frequency resolution and reduced PSLR. The proposed windows at $\alpha = 0.4$ are illustrated in Fig.8. The vertical axis represents the amplitude; the horizontal axis represents the time normalized by the frequency; and the red, blue, and green lines are the proposed windows 5, 6, and 7, respectively. Both ends of the proposed windows were emphasized. Therefore, the proposed windows emphasize the waveform discontinuity.

C. EVALUATION RESULTS

In this subsection, the evaluation results for the proposed windows are presented. Table 2 lists the design and evaluation results of the proposed windows. To understand the

TABLE 2. Evaluation results of proposed windows 5, 6, and 7.

window	α	β	γ	3dB width	Main-lobe width	PSLR [dB]	ISLR [dB]
Rectangular	0	-	-	0.888	2	-13.26	-9.68
Proposed 5	0.2	-	-	0.86	1.917	-11.90	-8.19
Proposed 5	0.4	-	-	0.826	1.810	-10.27	-6.41
Proposed 5	0.6	-	-	0.783	1.685	-8.31	-4.24
Proposed 5	0.8	-	-	0.73	1.535	-5.87	-1.53
Proposed 5	0.95	-	-	0.679	1.4	-3.59	1.05
Proposed 6	0	0.16	-	0.92	2.157	-17.04	-11.12
Proposed 6	0.2	0.16	-	0.893	2.059	-15.55	-9.60
Proposed 6	0.4	0.17	-	0.861	1.953	-14.00	-7.84
Proposed 6	0.6	0.18	-	0.82	1.822	-11.98	-5.67
Proposed 6	0.8	0.2	-	0.767	1.665	-9.54	-2.90
Proposed 6	0.95	0.22	-	0.715	1.516	-7.16	-0.16
Proposed 7	0	0.23	0.07	0.947	2.278	-19.47	-12.16
Proposed 7	0.2	0.23	0.08	0.922	2.184	-18.15	-10.71
Proposed 7	0.4	0.24	0.09	0.893	2.082	-16.70	-8.99
Proposed 7	0.6	0.25	0.09	0.852	1.945	-14.65	-6.76
Proposed 7	0.8	0.26	0.09	0.796	1.765	-11.77	-3.84
Proposed 7	0.95	0.28	0.1	0.744	1.608	-9.30	-1.01

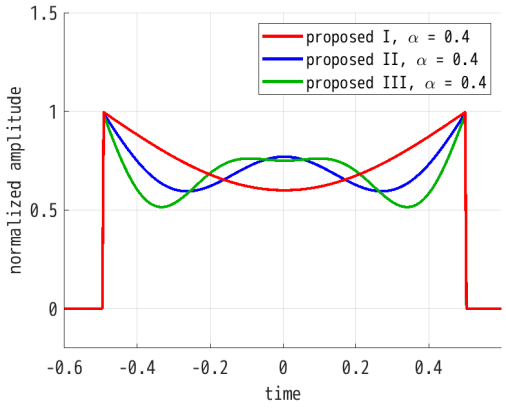

FIGURE 8. Proposed windows 5, 6, and 7($\alpha = 0.4$).

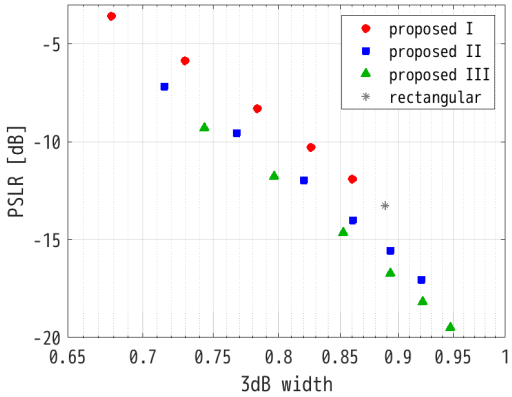

FIGURE 9. PSLR versus 3 dB width of the proposed windows 5, 6, and 7.

performance of the proposed windows, we evaluated the 3 dB width, main lobe width, PSLR, and ISLR. For visual understanding, Fig. 9 and 10 show the changes in PSLR and ISLR, respectively, where the scatter plots are plotted with PSLR and ISLR on the vertical axis and the 3 dB width on the horizontal axis. In each figure, the plots of proposed windows 5, 6, and 7 are indicated by red circles, blue squares, and green triangles, respectively. For comparison, the plots of the rectangular window, which is the best frequency resolution in conventional windows, are represented by gray stars. In the proposed windows, the discontinuity of the waveform was emphasized with respect to the increase in α, while the frequency resolution was improved, and the sidelobes were increased. Next, we confirmed PSLR and ISLR. The PSLR improves in the order of proposed windows 7, 6, and 5, whereas, the ISLR deteriorates in the order of proposed windows 7, 6, and 5. A reduction in PSLR causes deterioration of the ISLR. The normalized power profiles at $\alpha = 0.4$ are shown in Fig.11 and 12. The vertical axes represent the normalized power, the horizontal axes represent the frequency normalized by time, the gray lines represent the sinc functions, and the red, blue, and green lines represent the profiles of the proposed windows 5, 6, and 7, respectively. In the profiles of the proposed windows 5 and 6, the main lobes are narrower than those of the sinc function. In particular, the profile of proposed window 6 can improve the frequency resolution and PSLR simultaneously. In the profile of proposed window 7, the 3 dB-width is almost the same as the sinc function; however, the PSLR improves. Furthermore, it should be noted that the level of the sidelobes apart from the main lobe rises because the main lobe is mainly reduced by the term $\cos(\pi x)$.

One application of these proposed windows is super-resolution of imaging radar and other. We have used them for super-resolution of synthetic aperture radar images to confirm the effect. The details will be reported in a later article.

IV. WINDOW FUNCTIONS DESIGNED IN ADVANCE REDUCING THE SIDELOBES FURTHER

A. DESIGN GUIDELINE

The Hamming window is a typical cosine-sum window. The following function was proposed to reduce sidelobes with respect to the Hamming window [21]:

$$w_{\text{conv5}}(x) = (1 - \alpha - \beta) + \alpha \cos(2\pi x) + \beta \cos(6\pi x) \quad (12)$$

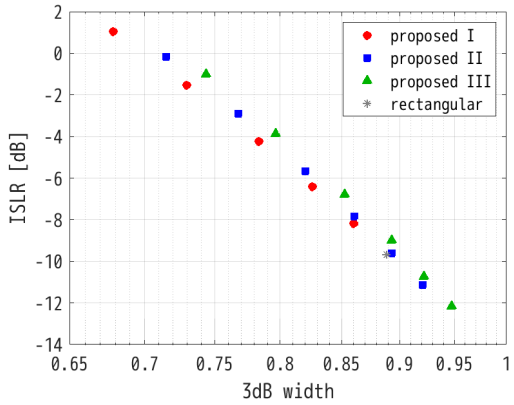

FIGURE 10. ISLR versus 3 dB width of the proposed windows 5, 6, and 7.

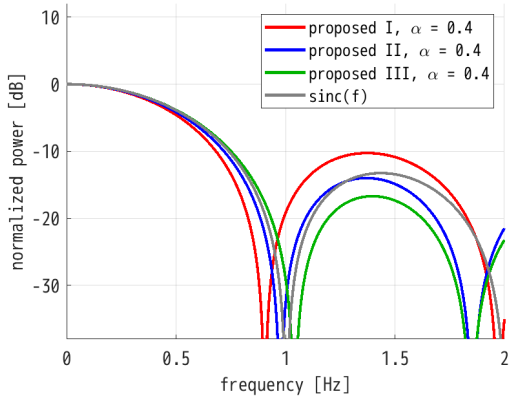

FIGURE 11. Power profile of the proposed windows 5, 6, and 7 with zoom.

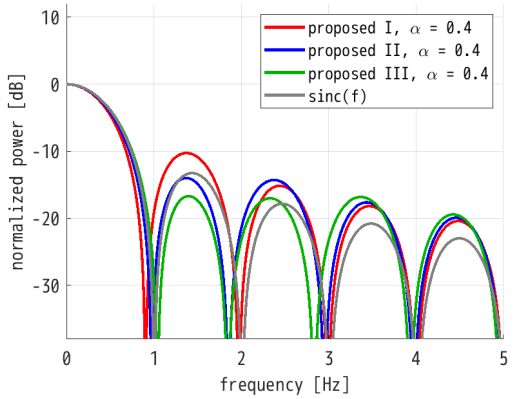

FIGURE 12. Power profile of the proposed windows 5, 6, and 7 with wide.

α and β are real numbers. We call this window the conventional window 5. The feature of this window is that the term $\cos(4\pi x)$ is not included. As a result, the sidelobes are reduced by the term $\cos(6\pi x)$ without degrading the frequency resolution. However, in the case of the general Hamming window, which is obtained by generalizing the coefficient of the Hamming window, the term $-\cos(4\pi x)$ may reduce the sidelobes without degrading the frequency resolution. This aspect should be considered in future studies.

Accordingly, we propose a window function that reduces the sidelobes in the generalized Hamming window without degrading the frequency resolution. The feature of the proposed window is that it contains the term -cos($4\pi x$) with a negative coefficient, which is different from conventional cosine-sum windows. The sidelobe decay of the generalized Hamming window was -6 dB/oct.; however, we focus on the window function, which is -12 dB/oct. and make a similar proposal.

B. PROPOSED WINDOWS

When $-0.5 \leq x \leq 0.5$, the frequency component of the constant term in the window function is a sinc function. The sinc function is -6 dB/oct. The following generalized Hamming window function is used to freely design and reduce the sidelobes of the sinc function.

$$w_{\text{ham}} = (1-\alpha) + \alpha\cos(2\pi x) \tag{13}$$

Because $\cos(2\pi x)$ is -6 dB/oct., the sidelobe decay was not damaged. This window is an application of the sidelobe reduction principle in Eq. (8). Let $F_x[](f)$ represent the transformation of a function for x to frequency f. $f_x[\cos(2\pi x)](f)$ is given by the sum of the sinc functions shifted by ± 1. The sinc function and $f_x[\cos(2\pi x)](f)$ overlap the null points. Because the occurrence positions of both sidelobes are in harmony, and their signs are reversed, the sidelobes of the generalized Hamming window are reduced. By adding a wide main lobe of $f_x[\cos(2\pi x)](f)$, the frequency resolution deteriorates, while reducing the first sidelobes of the sinc function. Consequently, as α increases, the sidelobes decrease and frequency resolution deteriorates.

However, when finding the window function with -12 dB/oct., we can use $\cos(\pi x)$. For this function, the reduction of sidelobes can be freely designed using the following equation:

$$w_{\text{hlf}} = (1-\alpha)\cos(\pi x) + \alpha\cos(3\pi x) \tag{14}$$

Because $\cos(3\pi x)$ is also -12 dB/oct., its sidelobe decay was $-$ -12 dB/oct. As α increases, the sidelobes decrease and the frequency resolution deteriorates. In this study, the window function is called the generalized half-cosine window. We also propose a reduction in the sidelobes relative to the generalized half-cosine window.

In this study, we attempted to reduce the sidelobes of the generalized Hamming window by designing a window function as

$$w_{\text{pro8}}(x) = (1-\alpha) + \alpha\cos(2\pi x) - \beta\cos(4\pi x) + \gamma\cos(6\pi x), \tag{15}$$

where γ denotes a positive real number. This window is called the proposed window 8. The feature of the proposed method is that the sign of the coefficient $\cos(4\pi x)$ is inverted,

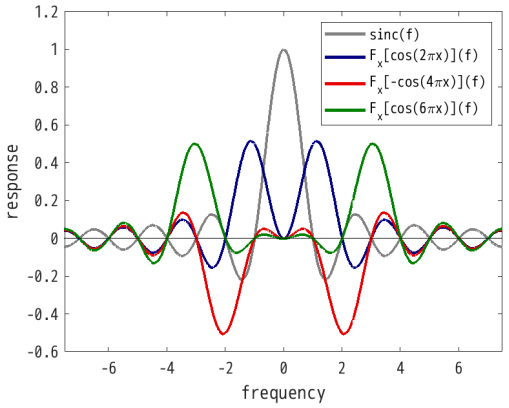

FIGURE 13. Frequency response of $\cos(2\pi x)$, $-\cos(4\pi x)$, and $\cos(6\pi x)$.

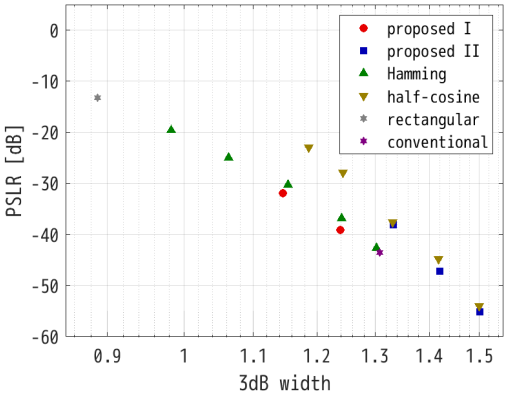

FIGURE 14. PSLR versus 3 dB width of the proposed windows 8 and 9.

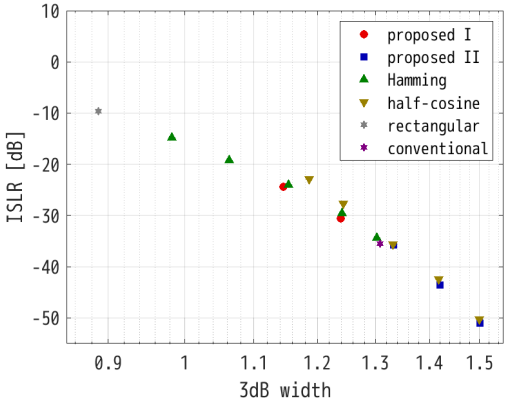

FIGURE 15. ISLR versus 3 dB width of the proposed windows 8 and 9.

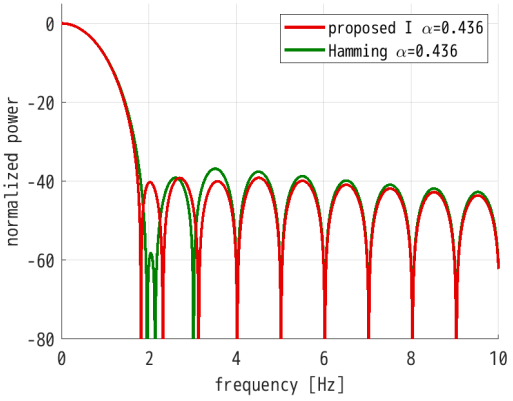

FIGURE 16. Power profile of the proposed window 8 ($\alpha = 0.436$).

which is different from conventional windows. This window function is designed by determining α which forms the desired frequency resolution, and then additionally determining β and γ which can reduce sidelobes in the frequency region. To confirm the background of this method, the sinc functions $F_x[\cos(2\pi x)](f)$, $F_x[\text{-}\cos(4\pi x)](f)$, and $F_x[\cos(6\pi x)](f)$ are shown in Fig.13. In Fig.13, the horizontal axis represents the frequency, the vertical axis represents the response, the gray line represents the sinc function, the blue line represents $F_x[\cos(2\pi x)](f)$, the red line represents $F_x[\text{-}\cos(4\pi x)](f)$, and the green line represents $F_x[\cos(6\pi x)](f)$. Focusing on the sidelobes, which are sufficiently distant from each main lobe, the signs of the sidelobes in $F_x[\cos(2\pi x)](f)$, $F_x[\text{-}\cos(4\pi x)](f)$, and $F_x[\cos(6\pi x)](f)$ are all inverted with respect to that of the sidelobes in the sinc function. In some cases, further reduction of sidelobes can be expected by adding $F_x[\cos(2\pi x)](f)$, $F_x[\text{-}\cos(4\pi x)](f)$, and $F_x[\cos(6\pi x)](f)$ rather than adding only $F_x[\cos(2\pi x)](f)$ to the sinc function. However, by adding the main lobes of $F_x[\text{-}\cos(4\pi x)](f)$ to the sinc function, the first side lobes of the sinc function are excessively increased, whereas the second side lobes of sinc function are excessively decreased. To prevent the increase in the first sidelobes of the sinc function, we should provide an appropriate coefficient and add the term $F_x[\text{-}\cos(4\pi x)]\,(f)$. Therefore, β should be set according to the number of first sidelobes reduced by the main lobes of $F_x[\alpha\cos(2\pi x)]\,(f)$. Similarly, we adjust γ according to the number of second sidelobes reduced by $F_x[\alpha\cos(2\pi x)$ $\text{-}\beta\cos(4\pi x)](f)$. The proposed window 8 reduced the sidelobes of the generalized Hamming window. Because β and γ are small, the degradation in the frequency resolution is small.

We can design a generalized half-cosine window in the same manner. The proposed window 9 can be expressed as follows:

$$w_{\text{pro9}}(x) = (1-\alpha+\beta-\gamma)\cos(\pi x) + \alpha\cos(3\pi x) - \beta\cos(5\pi x) + \gamma\cos(7\pi x) \quad (16)$$

The coefficients of this window are determined in the same manner as in the proposed window 8. This window reduces the sidelobes of the generalized half-cosine window.

C. EVALUATION RESULTS

In this subsection, the evaluation results for the proposed windows are presented. Table 3 lists the design and evaluation results of the proposed windows. We evaluated the 3dB width, main lobe width, PSLR, and ISLR to evaluate

TABLE 3. Evaluation results of proposed windows 8 and 9.

window	α	β	γ	3dB width	Main-lobe width	PSLR [dB]	ISLR [dB]
Rectangular	-	-	-	0.888	2	-13.26	-9.68
Hamming	0.22	-	-	0.982	2.368	-19.52	-14.81
Hamming	0.32	-	-	1.063	2.753	-25.02	-19.2
Hamming	0.39	-	-	1.153	3.319	-30.31	-24.04
Proposed 8	0.39	0.019	-	1.145	3.128	-31.87	-24.4
Hamming	0.436	-	-	1.242	3.923	-36.82	-29.58
Proposed 8	0.436	0.01	0.005	1.239	3.641	-39.12	-30.61
Hamming	0.46	-	-	1.302	3.983	-42.66	-34.33
Conventional 5	0.46	-	0.004	1.308	3.985	-43.56	-35.44
half-cosine	-	-	-	1.187	3	-23	-22.94
half-cosine	0.06	-	-	1.243	3.301	-27.91	-27.73
half-cosine	0.127	-	-	1.332	3.898	-37.61	-35.66
Proposed 9	0.127	0.002	-	1.333	3.873	-38.15	-35.79
half-cosine	0.173	-	-	1.419	4.741	-44.82	-42.5
Proposed 9	0.173	0.003	-	1.421	4.494	-47.2	-43.6
half-cosine	0.205	-	-	1.5	5	-54.06	-50.31
Proposed 9	0.205	-	0.001	1.5	5	-55.12	-51.02

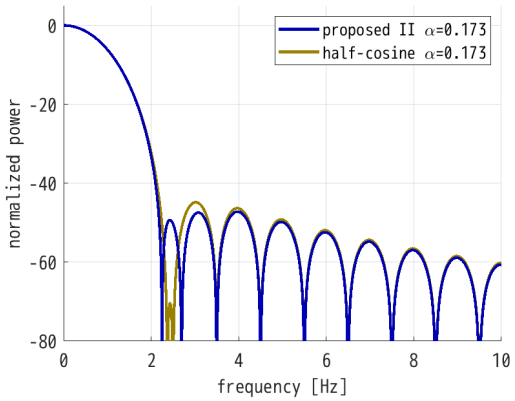

FIGURE 17. Power profile of the proposed window 9 ($\alpha = 0.173$).

the performance of the proposed windows. The proposed window improved the PSLR and ISLR as α increased. When the PSLR is confirmed, the proposed window 8 is improved by 2.3 dB at $\alpha = 0.436$, and the proposed window 9 is improved by 2.38 dB at $\alpha = 0.173$, respectively. However, the 3 dB width did not deteriorate significantly. On the other hand, when the mainlobe width is confirmed, the main lobe may be narrowed by proposed windows 8 and 9. For visual understanding of the improvement in PSLR and ISLR, Fig.14 and 15 show the scatter plots of PSLR and ISLR, respectively, with PSLR/ISLR on the vertical axis and the 3dB width on the horizontal axis. In each figure, the plots of proposed window 8, proposed window 9, generalized Hamming window, generalized half-cosine window, conventional window 5, and rectangular window are represented by red circles, blue squares, green triangles, yellow triangles, purple stars, and gray stars, respectively. The proposed windows 8 and 9 improve the generalized Hamming and generalized half-cosine windows, respectively.

In addition, the normalized power profiles were obtained to confirm the aspects of the sidelobes. The horizontal and vertical axes represent the frequency-normalized by time, and normalized power, respectively. Fig.16 shows the profiles of proposed window 8 and generalized Hamming window at $\alpha = 0.436$ with red and green lines, respectively. In the profile of the generalized Hamming window, the sidelobes were irregular. In contrast, the profile of proposed window 8 is in order and is reduced. Fig.17 shows the profiles of proposed window 9 and generalized half-cosine window at $\alpha = 0.173$ with blue and yellow lines, respectively. Again, the sidelobes of proposed window 9 are in order and are reduced.

V. CONCLUSION

In this study, we proposed window functions, which are extensions of cosine-sum windows, to achieve unprecedented performance. Furthermore, we present a design scheme for obtaining the window function by adding correction terms without damaging the sidelobe decay. At sidelobe decay of $-6, -12, -18, -24, -30$, and -36 dB/oct., we demonstrated excellent window functions for frequency resolution and PSLR. The window functions discussed here may improve the performance by increasing the number of terms. This design will be considered in future work.

REFERENCES

[1] F. J. Harris, "On the use of Windows for harmonic analysis with the discrete Fourier transform," *Proc. IEEE*, vol. 66, no. 1, pp. 51–83, Jan. 1978, doi: 10.1109/PROC.1978.10837.
[2] R. G. Kulkarni, "Synthesis of a new signal processing window," *Electron. Lett.*, vol. 55, no. 20, pp. 1108–1110, Oct. 2019, doi: 10.1049/el.2019.2116.
[3] G. V. Zaytsev and A. D. Khzmalyan, "A family of optimal Windows for harmonic analysis with arbitrary falloff rate of spectrum sidelobes," in *Proc. Int. Conf. Eng. Telecommun. (EnT)*, Nov. 2019, pp. 1–5, doi: 10.1109/EnT47717.2019.9030552.
[4] J. Liu, W. Wang, and H. Song, "Optimization of weighting window functions for SAR imaging via QCQP approach," *Sensors*, vol. 20, no. 2, p. 419, Jan. 2020, doi: 10.3390/s20020419.

[5] W. H. F. Smith, "Spectral Windows for satellite radar altimeters," *Adv. Space Res.*, vol. 62, no. 6, pp. 1576–1588, Sep. 2018, doi: 10.1016/j.asr.2018.01.012.
[6] Y. Sun, Q. Liu, J. Cai, and T. Long, "A novel weighted mismatched filter for reducing range sidelobes," *IEEE Trans. Aerosp. Electron. Syst.*, vol. 55, no. 3, pp. 1450–1460, Jun. 2019, doi: 10.1109/TAES.2018.2871479.
[7] F. D. Enggar, A. M. Muthiah, O. D. Winarko, O. N. Samijayani, and S. Rahmatia, "Performance comparison of various windowing on FMCW radar signal processing," in *Proc. Int. Symp. Electron. Smart Devices (ISESD)*, Nov. 2016, pp. 326–330, doi: 10.1109/ISESD.2016.7886743.
[8] K. Adhikari and B. Drozdenko, "Design and statistical analysis of tapered coprime and nested arrays for the min processor," *IEEE Access*, vol. 7, pp. 139601–139615, 2019, doi: 10.1109/ACCESS.2019.2944109.
[9] M. Sahidullah and G. Saha, "A novel windowing technique for efficient computation of MFCC for speaker recognition," *IEEE Signal Process. Lett.*, vol. 20, no. 2, pp. 149–152, Feb. 2013, doi: 10.1109/LSP.2012.2235067.
[10] T. Backstrom, "Comparison of windowing in speech and audio coding," in *Proc. IEEE Workshop Appl. Signal Process. Audio Acoust.*, Oct. 2013, pp. 1–4, doi: 10.1109/WASPAA.2013.6701853.
[11] B. Chen, Y. Li, X. Cao,W. Sun, andW. He, "Removal of power line interference from ECG signals using adaptive notch filters of sharp resolution," *IEEE Access*, vol. 7, pp. 150667–150676, 2019, doi: 10.1109/ICACCI.2016.7732031.
[12] R. G. Kulkarni, "Polynomial Windows with fast decaying sidelobes for narrow-band signals," *Signal Process.*, vol. 83, no. 6, pp. 1145–1149, Jun. 2003, doi: 10.1016/S0165-1684(03)00019-7.
[13] T. H. Yoon and E. K. Joo, "A flexible window function for spectral analysis [DSP tips & tricks]," *IEEE Signal Process. Mag.*, vol. 27, no. 2, pp. 139–142, Mar. 2010, doi: 10.1109/MSP.2009.935422.
[14] D. Chakraborty and N. Kovvali, "Generalized normal window for digital signal processing," in *Proc. IEEE Int. Conf. Acoust., Speech Signal Process.*, May 2013, pp. 6083–6087, doi: 10.1109/ICASSP.2013.6638833.
[15] Y. Sun, Q. Liu, J. Cai, and T. Long, "A novel method for designing general window functions with flexible spectral characteristics," *Sensors*, vol. 18, no. 9, pp. 3081–3090, Sep. 2018, doi: 10.3390/s18093081.
[16] A. G. Deczky, "Unispherical Windows," in *Proc. ISCAS IEEE Int. Symp. Circuits Syst.*, vol. 2, May 2001, pp. 85–88, doi: 10.1109/ISCAS.2001.921012.
[17] A. Rowinska-Schwarzweller and M. Wintermantel, "On designing FIR filters using Windows based on Gegenbauer polynomials," in *Proc. IEEE Int. Symp. Circuits Systems*, vol. 1, Aug. 2002, pp. 413–416, doi: 10.1109/ISCAS.2002.1009865.
[18] M. Jaskula, "New Windows family based on modified legendre polynomials," in *Proc. IMTC/. Proc. 19th IEEE Instrum. Meas. Technol. Conf.*, vol. 1, Aug. 2002, pp. 553–556, doi: 10.1109/IMTC.2002.1006902.
[19] K. Avci and A. Nacaroglu, "Cosine hyperbolic window family with its application to FIR filter design," in *Proc. 3rd Int. Conf. Inf. Commun. Technol., Theory Appl.*, Apr. 2008, pp. 1–6, doi: 10.1109/ICTTA.2008.4530047.
[20] M. G. Shayesteh and M. Mottaghi-Kashtiban, "FIR filter design using a new window function," in *Proc. 16th Int. Conf. Digit. Signal Process.*, Jul. 2009, pp. 1–6, doi: 10.1109/ICDSP.2009.5201209.
[21] M. Kashtiban and M. Shayesteh, "New efficient window function, replacement for the Hamming window," *IET Signal Process.*, vol. 5, no. 5, pp. 499–505, Aug. 2011, doi: 10.1049/iet-spr.2010.0272.
[22] J. F. Justo and W. Beccaro, "Generalized adaptive polynomial window function," *IEEE Access*, vol. 8, pp. 187584–187589, 2020, doi: 10.1109/ACCESS.2020.3030903.
[23] K. Okarma, "Polynomial Windows with low sidelobes' level," *Signal Process.*, vol. 87, no. 4, pp. 782–788, Apr. 2007, doi: 10.1016/j.sigpro.2006.09.007.
[24] C. M. Zierhofer, "Data window with tunable side lobe ripple decay," *IEEE Signal Process. Lett.*, vol. 14, no. 11, pp. 824–827, Nov. 2007, doi: 10.1109/LSP.2007.901696.
[25] C. Helmrich and R. Geiger, "Signal processor window provider, encoded media signal, method for processing a signal and method for providing a window," U.S. Patent 8 907 822, Sep. 11, 2012.
[26] G. V. Zaytsev and A. D. Khzmalyan, "A family of optimal window functions for spectral analysis with the spectrum sidelobe falloff rate multiple of 12 dB per octave," *J. Commun. Technol. Electron.*, vol. 65, no. 5, pp. 502–515, May 2020, doi: 10.1134/S1064226920050137.
[27] R. M. Rodríguez-Dagnino, "Mathieu Windows for signal processing," *Circuits, Syst., Signal Process.*, vol. 38, no. 6, pp. 2736–2766, Jun. 2019, doi: 10.1007/s00034-018-0989-z.
[28] A. Noureddine, M. Boussif, and C. Adnane, "A modified ultraspherical window and its application for speech enhancement," *Traitement du Signal*, vol. 39, no. 1, pp. 79–86, Feb. 2022, doi: 10.18280/ts.390108.
[29] T. Wang, J. Liang, Y. Tu, H. C. So, and Y. Li, "Window function design via fractional programming," *Digital Signal Process.*, vol. 132, pp. 1–9, Dec. 2022, doi: 10.1016/j.dsp.2022.103785.

TOMOYA YAMAOKA received the B.S., M.S., and Ph.D. degrees from Nagoya University, Nagoya, Japan, in 2004, 2006, and 2016, respectively.

He joined Mitsubishi Electric Corporation, Tokyo, in 2006, where he has been engaged in research and development on radar signal processing and wireless communication systems. He is currently a Researcher with the Information Technology Research and Development Center, Mitsubishi Electric Corporation, Kamakura, Japan.

SATOSHI KAGEME received the master's degree from the Tokyo University of Science, Tokyo, Japan, in 1999.

He joined Mitsubishi Electric Corporation, Tokyo, in 1999, where he has been engaged in research and development on radar signal processing and radar systems. He is currently an Engineer with the Kamakura Works, Mitsubishi Electric Corporation, Kanagawa, Japan.